Absorption, luminescence, resonance Raman, and resonance coherent anti-Stokes Raman spectroscopy on unsymmetrically substituted diacetylene single crystals with color zones

ARTICLE *in* THE JOURNAL OF CHEMICAL PHYSICS · AUGUST 1992

Impact Factor: 2.95 · DOI: 10.1063/1.463115

3 AUTHORS, INCLUDING:

Arnulf Materny
Jacobs University
198 PUBLICATIONS **2,336** CITATIONS
SEE PROFILE

Wolfgang Kiefer
University of Wuerzburg
881 PUBLICATIONS **9,877** CITATIONS
SEE PROFILE

Absorption, luminescence, resonance Raman, and resonance coherent anti-Stokes Raman spectroscopy on unsymmetrically substituted diacetylene single crystals with color zones

A. Materny and W. Kiefer
Institut für Physikalische Chemie der Universität Würzburg, Marcusstrasse 9-11, W-8700 Würzburg, Germany

M. Schwoerer
Physikalisches Institut der Universität Bayreuth and Bayreuther Institut für Makromolekül-Forschung, P. O. Box 101251, W-8580 Bayreuth, Germany

(Received 3 January 1992; accepted 28 April 1992)

We have analyzed the color zones in single crystals of the diacetylene derivative 6-(*p*-toluenesulfonyloxy)-2,4-hexadiynyl-*p*-fluorobenzenesulfonate by means of various optical spectroscopical methods in order to derive a plausible model for the origin of this type of chromism. By applying absorption, luminescence, resonance Raman, and coherent anti-Stokes Raman spectroscopy we obtained sufficient information for an understanding of the nature of the color zones. With the help of a nearly free-electron model calculation and a theoretical model for side group torsions, we found that a disturbance of the π-electron conjugation by a defect hindrance on side groups is the proper reason for the observed chromism. Growth defects in {111} crystal-growth sectors with a Burgers vector in the [010] direction cause the shape of the color zones. We found, particularly, that resonance coherent anti-Stokes Raman spectroscopy proves to be a valuable tool for the investigation of electronic and structural properties of the diacetylene crystals.

I. INTRODUCTION

Due to their nonlinear properties diacetylene polymers (PDA's), together with a series of other conjugated materials, are candidates for future applications in optoelectronics or molecular electronics.[1] The large third-order nonlinear optical response in PDA crystals was first reported by Sauteret *et al.*[2] The third-order susceptibilities $\chi^{(3)}$ of the polymerized crystals reach values comparable to those of inorganic semiconductors. The diversity of substitutional sidegroups has enabled a large number of PDA's to be synthesized, since the discovery of this type of polymerized crystal by Wegner.[3] Most PDA's are symmetrically substituted and, therefore, show centrosymmetric symmetry, which yields a zero second-order susceptibility $\chi^{(2)}$. The hope to obtain noncentrosymmetric structures which provide nonlinear optical effects initiated the synthesis of unsymmetrically substituted diacetylenes. Recently, the asymmetric diacetylene derivative 6-(*p*-toluenesulfonyloxy)-2,4-hexadiynyl-*p*-fluorobenzenesulfonate (TS/FBS) was synthesized[4,5] which is unsymmetrically substituted with the side groups of the well-known symmetric diacetylenes 2,4-hexadiynylene-di-*p*-toluenesulfonate (TS6) (Ref. 6) and 2,4-hexadiynylene-di-*p*-fluorobenzenesulfonate (FBS) (Ref. 7) (see Table I). The diacetylene monomers (DA's) of the three diacetylenes TS6, FBS, and TS/FBS undergo a topochemical solid-state polymerization when treated with heat or high-energy radiation (UV, γ, x ray or e^-). From this reaction, which is shown in Fig. 1, polymer chains arise, which have a substantial π-electron delocalization, forming a nearly one-dimensional electronic system. There exist two mesomeric structures for the resulting polymer backbone. Figure 1(a) shows the acetylenic and Fig. 1(b) shows the butatrienic form. From the crystal parameters of TS/FBS PDA's,[5] it follows that the acetylenic form is the preferred one, similar to TS6 and FBS. In a first investigation of TS/FBS, the single reaction steps and intermediates of the solid-state polymerization have been discussed.[8]

DA crystals of TS/FBS show a slight pink color which is due to an initial low polymer content produced during the crystal growth process. The polymer chains are embedded in the monomer matrix being all parallel to the crystal *b* axis of the monomeric crystal lattice (see Fig. 2). The absorption spectrum of such crystals (subsequently referred to as *P* absorption) shows a band with a 0-0 transition at about 16 800 cm^{-1} followed by a vibronic structure extending to the high-energy side. Solid-state polymerization results in PDA crystals having nearly 100% conversion. These TS/FBS PDA crystals show a metallic luster. Often TS/FBS DA crystals have a different appearance:[9] Sharply separated color zones can be seen which usually resemble a "butterfly" shape. These yellow to orange colored areas are schematically shown in Fig. 2 as speckled arrays. Such color zones were found also in TS6 and FBS DA crystals.[8] In absorption they

TABLE I. Substituents of TS6, FBS, and TS/FBS diacetylenes.

Diacetylene	Substituent
TS6	$R = R'$:–CH_2–O–SO_2–⬭–CH_3
FBS	$R = R'$:–CH_2–O–SO_2–⬭–F
TS/FBS	$R \equiv$ TS6, $R' \equiv$ FBS

 0021-9606/92/162237-10$06.00

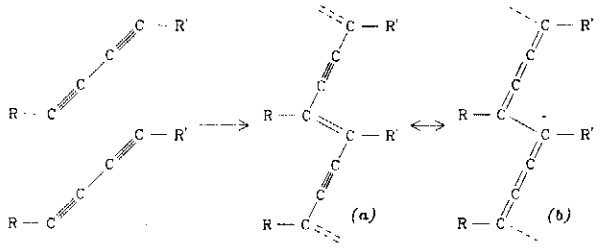

FIG. 1. Topochemical solid-state polymerization of diacetylene monomers with mesomeric backbone structures of the polymer: (a) acetylenic and (b) butatrienic form.

show a band which is blue-shifted relative to the P band (Y absorption) and which contains a vibronic structure.[8] Reversible and irreversible chromisms of various forms were reported in the last 15 years for many diacetylenes. The different kinds were investigated by various methods in solutions of PDA's,[10,11] in crystals,[12,13] and in thin films.[14,15] Primarily optical spectroscopy has been performed to gain more knowledge of the nature of the chromism. Thin film studies were undertaken mainly to investigate the nonlinear properties of the different chromatic forms of the PDA's.[16,17] Despite these extensive studies, the molecular mechanism giving rise to the chromic transition is still a controversial subject. A proposition that a change between two mesomeric structures causes the observed color changes[18] seems unlikely in lieu of recent experimental and theoretical results.[19] Interruptions of the conjugation length of the polymer backbones are now the most commonly accepted reason for chromism effects. This assumption already goes back to 1976 (Ref. 12) and the main question which still remains is what kind of interruptions may cause this effect. Most probably different kinds of chemical or configurational defects are the main cause for a planar-to-nonplanar transition of the PDA chains. This would result in a shortening of the parts of the chain where a continuous delocalization of the π-electrons is possible. Such a shortening of the conjugation length would explain shifts in the absorption to higher energies.

The color zones in TS/FBS were already characterized by absorption (see the aforementioned) and luminescence spectroscopy. Preliminary results are published elsewhere.[8] In this paper we intended to perform a more accurate investigation of the color zones in TS/FBS DA crystals by making use of several optical spectroscopy methods. More evidence of the structural and electronic nature of the Y zone should be gained by applying these methods to the same crystals. Here, we present results from absorption, luminescence, resonance Raman, and resonance coherent anti-Stokes Raman scattering (CARS) spectroscopy. The results are discussed in comparison to other forms of chromism and to results we already obtained for FBS DA crystals.[20] A theoretical interpretation of absorption, resonance Raman and resonance CARS spectra for the P-form DA crystals by means of a Franck–Condon calculation has partly been accomplished.[21,22] Similar calculations for Y-zone spectra are in progress.[20]

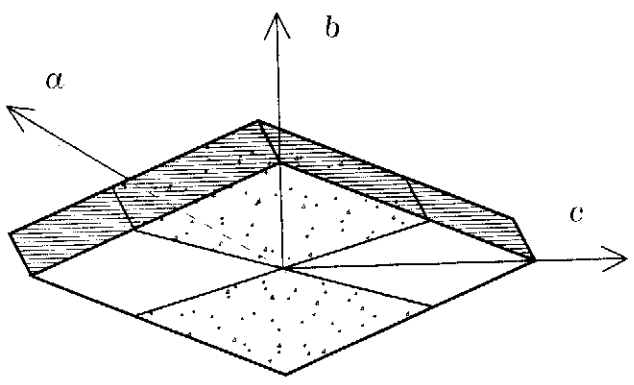

FIG. 2. Schematic form of FBS, TS/FBS, or TS6 single crystals. Arrows indicate crystal axes of the monoclinic lattice. The speckled areas show a typical shape of the yellow color zones (Y zone).

II. EXPERIMENT

The unsymmetrically substituted TS/FBS DA was synthesized according to methods described by Strohriegl[4] and by Bertault.[5] The lozenged monoclinic crystals were obtained from solution and had less than 1% polymer content. The freshly grown DA crystals were cleaved parallel to the {100} surface (containing b and c axis, see Fig. 2). The resulting thin platelets were about 50 μm thick and about 3 mm long in the chain direction ($\| b$ axis). After cleaving, the TS/FBS DA crystals were put into a cryostat and cooled to about 10 K. Cooling of the crystals was necessary because of the enormous heat sensitivity of the TS/FBS DA single crystals. The polarization of light was chosen to be parallel to the b axis. This was required due to the high optical anisotropy of the DA crystals, caused by the parallel polymer chains.

The experimental setup used for absorption and luminescence spectroscopy has been described elsewhere.[8] For resonance Raman spectroscopy we used a micro Raman setup.[23] We chose a backscattering arrangement, where the incident laser light was parallel to the {100} surface of the crystal. For the detection, an optical multichannel analyzer (OMA) detector was used, which allowed us to take large parts of the spectra at one time. The setup for the pulsed solid-state CARS measurements has also been described elsewhere in detail.[24] The simultaneous use of two dye lasers enabled us to perform scans of the Stokes laser frequency ω_s as well as the pump frequency ω_p. Therefore, resonance CARS spectroscopy was possible. The beam of the pump laser was aligned vertically to the {100} plane of the DA crystal. In order to excite specific phonons in the single crystals, the phase matching condition had to be fulfilled. This means that the difference between the pump and Stokes beam wave vector had to coincide with the wave vector of the coherently excited phonons in the crystals, i.e., $\mathbf{k}_p - \mathbf{k}_s = \mathbf{k}_{\text{phon}}$ (see Fig. 3). This was achieved by changing the crossing angle Θ between the pump and the Stokes beam as well as the orientation of the plane spanned by pump and Stokes beam, relative to the crystal b axis.

Before each Raman or CARS measurement we took an absorption spectrum of the P and Y zone. In all experiments a strict separation of P and Y zones of the TS/FBS DA crys-

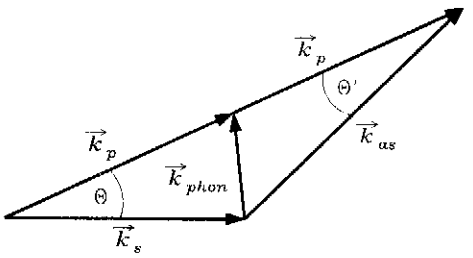

FIG. 3. Momentum (wave) vectors for the CARS process. $\mathbf{k}_p$, $\mathbf{k}_s$, and $\mathbf{k}_{as}$ are the momentum vectors of the pump, Stokes, and CARS beam, respectively. $\mathbf{k}_{phon}$ is the momentum vector for the phonon. Θ is the crossing (phase) and Θ' the collection angle.

tals was obtained by cleaving the crystals or by appropriate shielding of the *P* or *Y* zone. More details of the experimental part of our work are given in Sec. III together with results from spectroscopic measurements.

III. RESULTS AND DISCUSSION

The *Y* zones of TS/FBS have a color which can vary slightly from yellow to orange. These observations were also made for the other DA's, FBS, and TS6. This clearly shows that the electronic properties of the *Y* zone are not constant and may change from one crystal to another. A more exact characterization of the color zones can be given by absorption spectroscopy. Few crystals show relatively simple absorption behavior. Figure 4 shows such absorption spectra for the *P* zone [see Fig. 4(b)] and for the *Y* zone [Fig. 4(a)]. The absorption spectrum of the *P* zone shows the well-known absorption of the normal polymer chains embedded in the monomer matrix.[25] The *P* chains exhibit a structured absorption band consisting of a 0-0 transition at about 16 800 cm^{-1} and well-resolved vibronic lines. At about 30 000 cm^{-1} the absorption of the monomers starts, which becomes very strong in the ultraviolet region. The *P* band also shows up in the absorption spectrum of the *Y* zone [Fig. 4(a)], where it is weaker but also structured. The main feature in the *Y* absorption spectrum, however, is a very intense new band. This *Y* band is similar to the *P* band and also contains a 0-0 transition with vibronic sidebands, which is similar to that of the *P* band. From this observation we conclude that the origin of the *Y* absorption is due to polymer chains, too. Other measurements like the temperature dependence of the $^1A_g - {}^1B_u$ transitions for both bands confirm this assumption.[8] Most TS/FBS crystals, however, show an absorption spectrum which is not as well resolved as the one shown in Fig. 4. As an example we show in Fig. 5 such absorption spectra obtained from a TS/FBS DA crystal with color zones. In Fig. 5(b) the absorption spectrum of the *P* zone is shown. The vibronic structure can be recognized but is not as well resolved as in Fig. 4(b). The whole spectrum is broader and the 0-0 transition line shows a shoulder. Calculations for TS/FBS oligomers,[8] where the nearly-free-electron model (NFEM) calculation was used, showed that the $^1A_g - {}^1B_u$ energy depends on the length of the oligomer chains according to[12]

$$E_n = \frac{h^2}{8ml^2}(4n+1) + E_\infty\left(1 - \frac{1}{4n}\right) \tag{1}$$

with

$$l = na_1 + a_2, \tag{2}$$

where l is the length of the chain with n monomer units. a_1 is the length of a monomer unit and a_2 stands for the contribution of the chain ends. m is the electron mass and E_∞ is the transition energy for an infinite polymer chain. This model also yielded remarkable results for TS6 (Ref. 26) and for

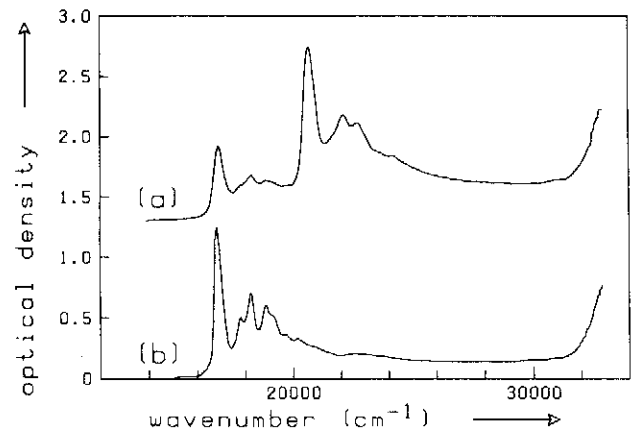

FIG. 4. Absorption spectra of a TS/FBS DA crystal with color zones and very regular shape recorded at a sample temperature of 10 K. The polarization of the transmitted light is parallel to the crystal *b* axis. The absorption spectrum of the (a) *Y* and of the (b) *P* zone (reproduced in part, from Ref. 8).

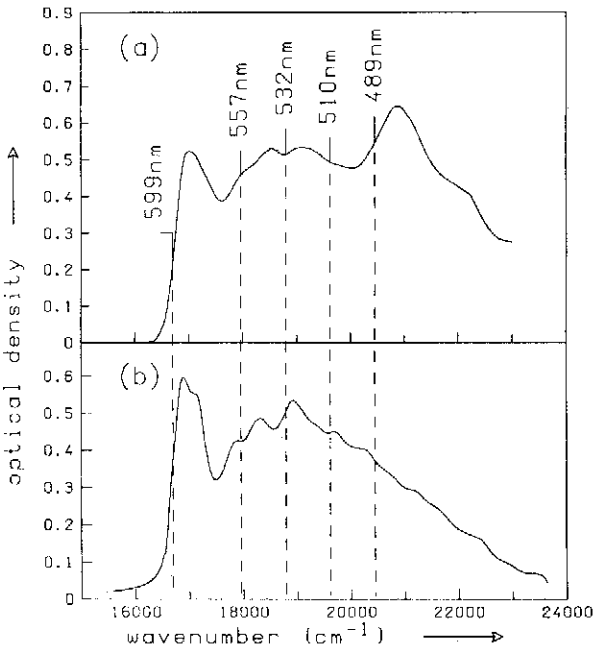

FIG. 5. Absorption spectra of a TS/FBS DA crystal with color zones and an average shape at a sample temperature of 10 K. The polarization of the transmitted light is parallel to the crystal *b* axis. The absorption spectrum of the (a) *Y* and of the (b) *P* zone. Vertical lines with numbers indicate wavelength positions of the pump laser, employed for excitation of the CARS spectra given in Fig. 10..

FBS (Ref. 27). Results obtained for a fit to the stable oligomer absorptions by varying a_2 and E_∞ are given in Table II and Fig. 6. Applying these results we found that the chains responsible for the P absorption in Fig. 5 are about 10–15 monomer units long. Chains of this length show discernible optical properties for different n. Therefore, if there would be a distribution of chain lengths which is broader than that responsible for the P absorption (Fig. 4), the analogous broader absorption in Fig. 5 could be explained. By inspecting crystals responsible for absorptions like those seen in Figs. 4 and 5, it is likely that the crystals which have broader spectra are not as perfectly shaped as those crystals which have spectra as seen in Fig. 4. Therefore, we suppose that there is a connection between crystal growth and chain length distribution. The spectrum for the Y zone in Fig. 5(a) is also very broad and unresolved. Only an absorption line at about 21 000 cm^{-1} can clearly be recognized. To gain more information regarding the electronic as well as the structural properties of the DA crystals and in consequence of the nature of the Y zones, we used additional spectroscopic methods.

Resonance Raman spectroscopy proved to be a powerful tool to investigate PDA and DA crystals.[28] Investigations of different kinds of chromism were already performed and yielded informative results.[11,12,15] Preliminary results from resonance Raman measurements on DA color zones were published some time ago.[23] However, we found that resonance Raman spectroscopy is a limited method for the investigation of color zones because of strong luminescence in the Y zones when excited by laser frequencies higher than that of the ^1A_g–^1B_u transition of the Y absorption. This luminescence has a pronounced vibronic structure.[8] The luminescence exhibits two bands. One of them is very strong and is nearly the mirror image of the Y absorption [Fig. 7(a)] while the other is weak and can be correlated with the P absorption [Fig. 7(b)]. Both vanish if the excitation is shifted to lower energies. This luminescence makes resonance Raman measurements impossible for excitations which could be of interest for an enhancement of the Y transitions. Thus, only two possibilities remain to provide information about the Y zones by means of resonance Raman spectroscopy. The first it to choose crystals with very intense color zones. In this case using red excitation, differences between P and Y spectra also can be observed.[23] A second possibility is to study crystals with only a weak Y zone. There the luminescence remains relatively weak and for shorter excitation wavelengths a spectrum also can be obtained. An example for this is shown in Fig. 8. The spectra are all taken from the Y zone. PDA chains, if resonantly enhanced, exhibit only a few Raman lines which all belong to symmetric A_g modes of the PDA backbone.[29] In the wave-number region from 3500 to 500 cm^{-1} only four prominent Raman lines, labeled ω_1 to ω_4, and about six combination frequencies can be seen under this condition.[30] In Figs. 8(a) and 8(b) we display parts of the resonance Raman spectrum for an excitation of 633 nm which is preresonant with the P absorption. In Fig. 8(a) the

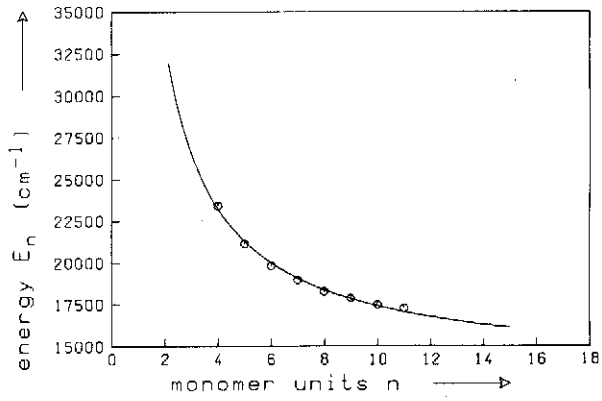

FIG. 6. ^1A_g–^1B_u 0-0 transition energies of the stable TS/FBS oligomers with chain length n (○). The sample temperature was about 10 K. The curve is a fit with the NFEM model (see text and Table II).

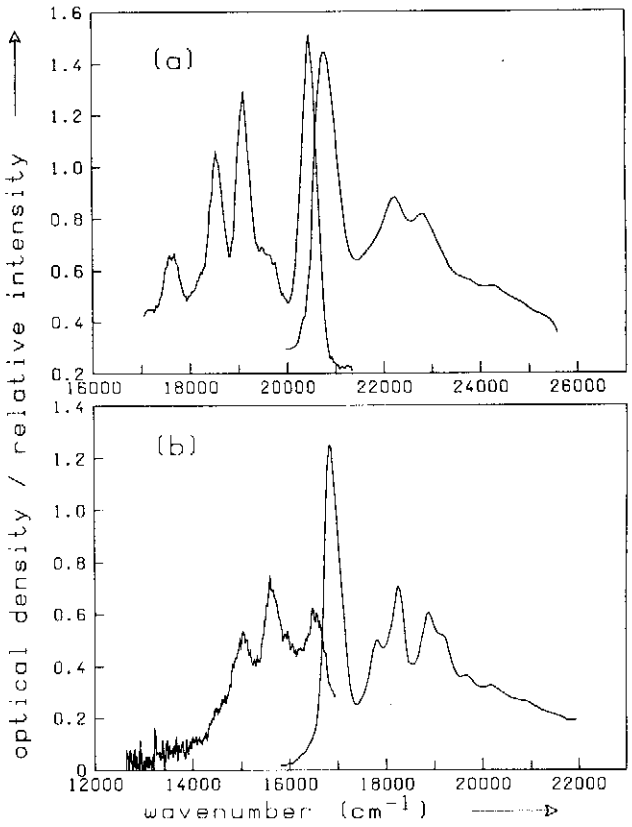

FIG. 7. Typical luminescence spectra of a Y zone of a TS/FBS DA crystal together with the associated absorption spectra. (a) The Y luminescence and absorption and (b) the P luminescence and absorption. The temperature of the sample was 10 K. Excitation wavelength was 325 nm. Polarization of incident and emitted light is parallel to the crystal b axis. (Reproduced from Ref. 8).

TABLE II. Parameters of the NFEM curve of Fig. 6 for the TS/FBS stable oligomer series SO_n. Parameters a_2 and E_∞ are obtained by a least-squares fit. a_1 was estimated taking data from x-ray crystal structure (Ref. 5).

Photoproduct series	a_1 (Å)	a_2 (Å)	E_∞ (cm^{-1})
SO_n	5.402	0.520	13573

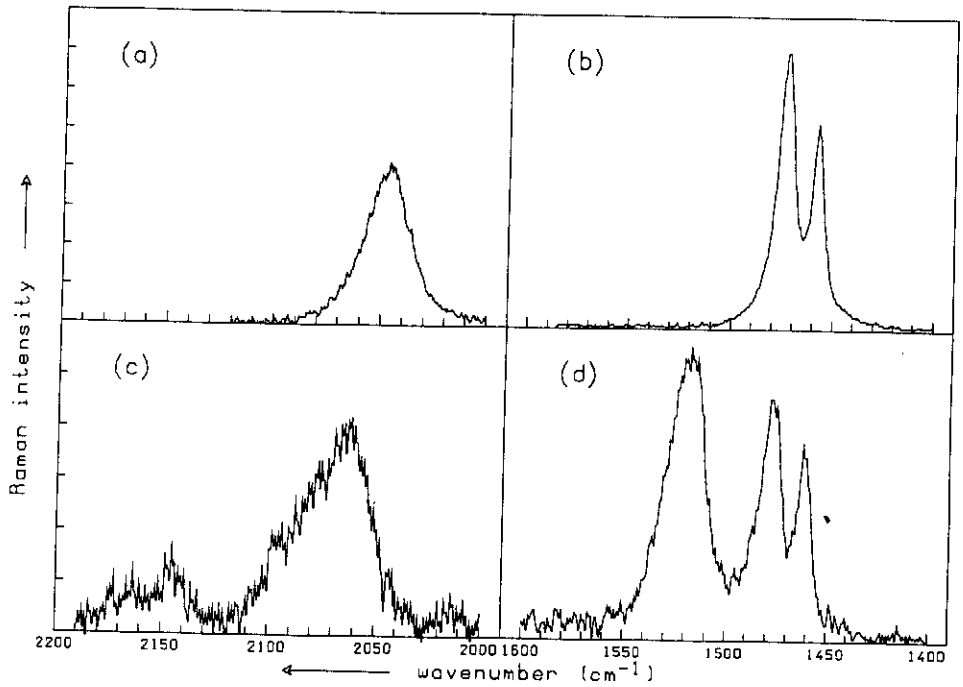

FIG. 8. Raman spectra of a TS/FBS DA crystal at 10 K, for excitation wavelength 633 nm [(a) and (b)] and 515 nm [(c) and (d)], taken in the Y zone. Polarization of incident and scattered light is parallel to the b axis of the crystal. Spectra on the left side [(a) and (c)] correspond to the C≡C stretching; those on the right side [(b) and (c)] correspond to the C=C stretching region of the P and Y zone. For further information see text.

ω_1 line (C≡C stretching) at about 2045 cm^{-1} is shown. In Fig. 8(b) a doublet can be seen at about 1475 cm^{-1}/1455 cm^{-1}. These Raman lines can be assigned to the ω_2 mode (C=C stretching) and to a Fermi resonance enhanced CH_2 scissors vibration (ω_{CH_2}) belonging to the sidegroup.[31] Because enhancement principally of the ^1A_g–^1B_u transition to the P chains is expected, we use the abbreviations ω_{1P} and ω_{2P}. Figures 8(c) and 8(d) show the same spectral regions for an excitation wavelength of 515 nm. The spectral lines are on top of an intense luminescence background which is not shown in Fig. 8. The ω_{2P} and ω_{CH_2} modes belonging to the P chains are slightly shifted to higher frequencies at about 1480 and 1460 cm^{-1}, respectively. In Fig. 8(a) a distinct new line shows up at about 1520 cm^{-1}. Because of the excitation near the Y absorption, we assign this Raman line to the C=C stretching vibration of the Y chains, subsequently called ω_{2Y}. In Fig. 8(c) the ω_{1P} line at 2045 cm^{-1} vanishes, but a new line can be seen at about 2060 cm^{-1}. We assign this line to the ω_{1Y} mode of the Y chains. Weak and noisy signals can be seen around 2140 to 2170 cm^{-1}. These could originate from the luminescence background or from additional lines belonging to the Y backbone. From the resonance Raman spectra obtained we are not able to obtain further information. This is due mainly to very strong luminescence, which does not allow a good evaluation of the resonance Raman spectra. Only with $\lambda_p = 515$ nm or longer excitation wavelengths have we been able to obtain Raman signals. Specifically, we are not able to assign the Y Raman lines to any concrete feature in the Y absorption spectrum.

A possibility to obtain resonance Raman spectra without any disturbing luminescence background would be to record anti-Stokes Raman spectra. These have already been obtained from PDA's.[32] However, the TS/FBS DA crystals are extremely sensitive to heating, because this leads to further polymerization and/or to destruction of the DA crystals. Therefore, laser irradiation with frequencies in resonance with the absorption of the polymer chains readily changes spectral conditions or even destroys the crystal. In particular, the Y zones seemed to be sensitive toward laser light. Even cooling the crystals to 10 K did not totally prevent spectral changes during the recording of Raman spectra. These changes could be easily observed using the OMA system. Both the observed changes as well as the necessity to cool the crystals made it impossible for us to obtain anti-Stokes Raman spectra of the TS/FBS crystals.

As mentioned earlier, the PDA polymer is an interesting material because of the large third-order nonlinear susceptibility $\chi^{(3)}$. Therefore, CARS spectroscopy seems to be a favorable method for obtaining anti-Stokes Raman spectra, which are free of luminescence. From the successful recording of CARS spectra of DA crystals of the P form we could assume that it may also be possible to obtain anti-Stokes Raman spectra for the materials discussed in this paper by this nonlinear coherent method.[24] For a detailed description of the CARS process we refer to other articles.[33,34] In short, the diagram in Fig. 9 shows a schematic energy representation of the CARS process. CARS is a four-wave mixing process using two equivalent laser frequencies (ω_p, pump laser frequency). The other two frequencies involved arise from the Stokes laser with the frequency ω_s and the coherent anti-Stokes Raman signal with frequency ω_{as}. CARS experiments for the P form DA crystals showed that a pronounced

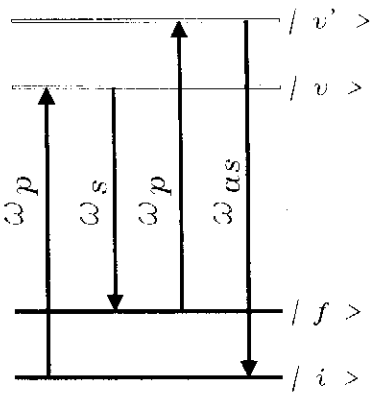

FIG. 9. Schematic representation of the CARS process. $|i\rangle$ and $|f\rangle$ are the initial and final state of the Raman process, respectively. $|v\rangle$ and $|v'\rangle$ are intermediate states of the CARS process. ω_p, ω_s, and ω_{as} are the frequencies of the pump, Stokes, and CARS beam, respectively.

resonance with the ^1A_g–^1B_u transitions of the delocalized π-electron system of the polymer backbone arises.[24]

From the aforementioned discussion it becomes clear that CARS experiments can only be performed with relatively low powers of the laser beams. Only with energies in the range 1 to 10 μJ could we avoid damage to the crystals when excitation in resonance with one of the 0-0 transitions was applied. Special care had to be taken for excitation in the Y zones. To confirm whether no damage of the crystals occured we repeated each measurement several times. A second problem was that both intensity and frequency of the CARS lines (analogous to the Raman lines) could shift considerably when the spot position on the crystal surface was changed. As mentioned earlier, short chains (up to 30 monomer units) do have discernible optical properties. If we presume that there is a distribution of relatively short chains in the monomer matrices of the TS/FBS DA crystals, inhomogeneities are to be expected. This explains the observed shifts. To obtain reliable CARS spectra, we therefore had to take spectra containing the ω_{1P}, $\omega_{2P}/\omega_{CH_2}$, and ω_{1Y},ω_{2Y} lines from one single-crystal spot. This means that we could not change the dyes of the tunable laser for such a measurement, since realignment of the beam would lead to a different focal spot on the crystal surface. Only if ω_p had to be changed other dyes were used and in this case we tried to irradiate nearly the same spot of the crystal surface. As a result, we could make use of only a few combinations of dyes for the pump and the Stokes laser which enabled us to take CARS spectra over a range of about 900 cm^{-1}.

To fulfill the phase matching conditions we had to pay attention to the following. First, the phase angle Θ had to be estimated. We found Θ to be in a range between 1°–3° without any measurable dispersion. Moreover, no difference was observed between P and Y zones. These experimental results are surprising because for such materials large phase angles and considerable dispersion are to be expected.[34] From PDA crystals it is known that the refractive index intrinsic to the polymers varies from 0 to 10 in the visible frequency region.[25] However, one has to consider that CARS spectroscopy is performed on DA crystals, which contain only a few polymer chains, which are embedded in a matrix of monomers. The TS/FBS monomers do not absorb in the visible region and, consequently, do not exhibit marked changes in the refractive index. Such a system is a solid solution having a low concentration of the polymer chains in the monomer matrix. Thus, the phase angle is determined by the monomers rather than by the polymer chains as long as the concentration is not too high.[35] This results in a small nearly constant phase angle for both the P and the Y zone CARS excitation. A further very strict condition which follows from the phase diagram shown in Fig. 3 is that the phonon momentum vector $\mathbf{k}_{phon}$ had to be chosen parallel to the b axis of the DA crystals. This means that $\mathbf{k}_{phon}$ must be parallel to the direction of the conjugated π-electron system of the polymer backbones. As already mentioned, the polarizations of the ω_p, ω_s, and ω_{as} beams were chosen to be parallel to the chains.

Figure 10 shows CARS spectra obtained from a TS/FBS DA crystal. The spectra were taken for different pump laser wavelengths λ_p, as labeled in Fig. 10. Figures 10(a) and 10(b) show CARS spectra taken in the P zone and Figs. 10(c)–10(l) show those taken from the Y zone of the crystal, respectively. For a comparison with the absorption spectra of the Y and P zone, we refer to Figs. 5(a) and 5(b), respectively. The excitation wavelengths λ_p used for the CARS spectroscopy are marked in the absorption spectra. The CARS spectra displayed are all corrected for different laser intensities, detection sensitivity and linearity, and also for absorption. For further details see Ref. 24.

The longest wavelength λ_p chosen for CARS was chosen at the Stokes side of the ^1A_g–^1B_u 0-0 transition of the P absorption ($\lambda_p = 599$ nm). Because of the reasons mentioned earlier, we did not succeed in taking CARS spectra in exact resonance with this transition. Figures 10(a) and 10(b) show the spectra for $\lambda_p = 599$ nm taken in the P zone of the TS/FBS DA crystal. Figure 10(a) clearly shows a doublet $\omega_{2P}/\omega_{CH_2}$ with associated wave numbers at about 1470 and 1455 cm^{-1} analogous to those found in the linear resonance Raman spectrum. The line shapes are typical for the resonance CARS spectroscopy.[36] The deep dip between the two adjacent lines (compare with the Raman spectra in Fig. 8) can be explained by considering the third-order susceptibility $\chi^{(3)}$ for such a doublet, written in a very simple form:

$$\chi^{(3)}_{\text{total}} = \chi^{(3)}_{\text{nr}} + \frac{\text{Re}\,\chi^{(3)}_{r_{2P}} + i\,\text{Im}\,\chi^{(3)}_{r_{2P}}}{\delta_{2P} - i\Gamma_{2P}} + \frac{\text{Re}\,\chi^{(3)}_{r_{CH_2}} + i\,\text{Im}\,\chi^{(3)}_{r_{CH_2}}}{\delta_{CH_2} - i\Gamma_{CH_2}} \tag{3}$$

with $\delta_{2P} = \omega_{2P} - (\omega_p - \omega_s)$ and $\delta_{CH_2} = \omega_{CH_2} - (\omega_p - \omega_s)$. $\chi^{(3)}_{\text{total}}$ is the total third-order nonlinear susceptibility for the CARS process involving the modes ω_{2P} and ω_{CH_2}. $\chi^{(3)}_{\text{nr}}$ contains the nonresonant, while Re $\chi^{(3)}_r$ and Im $\chi^{(3)}_r$ are the real and imaginary part of the resonant contributions to the third-order nonlinear susceptibility, respectively. Γ_{2P}

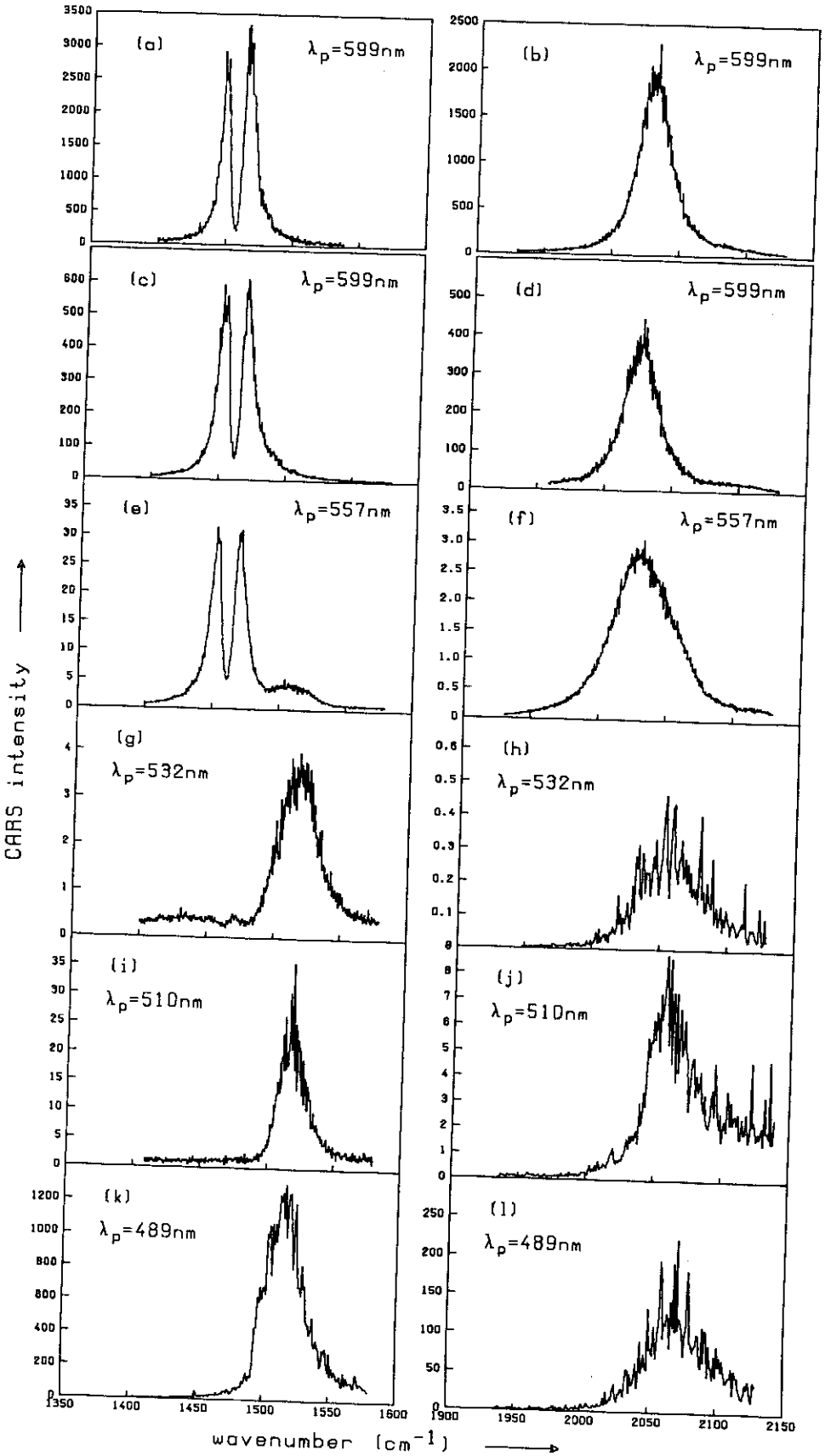

FIG. 10. Resonance CARS spectra of a TS/FBS DA crystal at 10 K. The pump wavelength λ_p used is labeled for each spectrum. For comparison with the absorption spectra of this crystal, see Fig. 5. (a) and (b) show CARS spectra of the P zone and (c)–(l) those for the Y zone. Spectra on the left side correspond to the C=C stretching region, those on the right side to the C≡C stretching region. For further details, see text.

and Γ_{CH_2} are the widths [full width at half maximum (FWHM)] of the two modes, considered. The intensity of the CARS signal is proportional to $|\chi^{(3)}_{\text{total}}|^2$ which contains two single expressions, one for each Raman peak, and also terms which can be designated as Raman–Raman cross terms for the two peaks. These cross terms are the reason for the observed deep dip between the two lines of the doublet. Figure 10(b) shows the ω_{1P} line at about 2030 cm^{-1} which is in coincidence with the results obtained from resonance Raman spectroscopy. The slight difference in absolute line positions between Raman spectra in Fig. 8 and CARS spectra in Fig. 10 is mainly due to the fact that the TS/FBS DA crystals used were not identical. Differences in Raman as well as absorption line positions are normal for different DA crystals because of the distinct chain length distributions. Lines intrinsic to the P zone are weaker by a factor of about 5, as compared to those of the Y zone, but appear at about the same frequencies as those intrinsic to the P zone. In Figs. 10(c) and 10(d) we display the $\omega_{2P}/\omega_{CH_2}$ and the ω_{1P} CARS lines, respectively, observed in the Y zone. Noticeable differences to the P spectra occur only for an excitation wavelength $\lambda_p = 557$ nm or shorter. In Fig. 10(e), besides the $\omega_{2P}/\omega_{CH_2}$ doublet, a weak shoulder appears at higher frequencies. The ω_{1P} line shown in Fig. 10(f) at about 2020 cm^{-1} exhibits only low intensity and is quite broad. In Figs. 10(g) and 10(h) new lines appear. In Fig. 10(g) only the $\omega_{2P}/\omega_{CH_2}$ doublet shows up. At about 1520 cm^{-1} a new line appears which is assigned to an ω_{2Y} mode. In Fig. 10(h) a weak line at about 2060 cm^{-1} can be seen. This line can be assigned to an ω_{1Y} mode. The wavelength λ_p chosen for the excitation of these spectra was 532 nm. In Figs. 10(i) and 10(j) and 10(k) and 10(l), the CARS spectra obtained for $\lambda_p = 510$ nm and $\lambda_p = 489$ nm, respectively, are shown. We observed strong resonance behavior of the CARS intensities while approaching the absorption line at about 480 nm (21 000 cm^{-1}) [see Fig. 5(a)] with the pump laser wavelength λ_p. In Figs. 10(g)–10(l) no resonance enhancement of any other CARS line was observed. This indicates that there is most likely no further ^1A_g–^1B_u 0-0 transition in addition to the one at about 21 000 cm^{-1}. Choosing $\lambda_p = 489$ nm we placed the excitation wavelength close to the absorption maximum at about 21 000 cm^{-1}. For this λ_p we succeeded in taking CARS spectra only after several attempts, without destroying the crystal. The observed ω_{2Y} and ω_{1Y} lines [see Figs. 10(k) and 10(l)] are very intense. The relatively high noise in these spectra is due to the fact that we had to reduce the laser powers to very low values. Therefore, the absolute intensities of the CARS lines were rather low. In the region 489 nm $> \lambda_p >$ 460 nm it was not possible to obtain CARS spectra, without rapid loss in line intensity, which suggests that an irreversible change in the material took place. The observed line positions, however, remained at about the same frequencies as those observed for excitation using $\lambda_p < 557$ nm. We therefore suppose that the 0-0 transition at about 21 000 cm^{-1} is the only one belonging to the Y chains in this particular TS/FBS crystal. Moreover, in other TS/FBS crystals, we could not find any additional features in the Y zone absorption. The only difference was the variation of the vibronic structure, as shown in Figs. 4 and 5. From this we believe that the Y chains existing in TS/FBS crystals are all of the same form. This is in contrast to observations made for Y zones in FBS, where different ^1A_g–^1B_u transitions were found for the Y chains.[20]

Our measurements strongly support the model which explains chromism effects in terms of a change in the conjugation length of the polymer backbone's π-electron system. The DA crystals allow the study of the effect of chain and conjugation length. The chains are well separated in the monomer matrix. The color effects in these crystals therefore should be a single-chain phenomenon[37] rather than a result of any form of aggregation.[38] The results of the NFEM calculation show that for the P chains in the TS/FBS DA crystal investigated, conjugation lengths of about 10 to 15 monomer units are to be expected. From x-ray structure analysis[5] we know that the P chains in DA crystals are planar and normally undisturbed. From this we conclude that the conjugation length and the chain length in the P chain backbones are about the same. Crystal-growth conditions determine whether polymer chain growth proceeds more or less homogeneously. This results in different widths of the chain length distribution. The absorption spectra in Figs. 4(b) and 5(b) strongly support this interpretation. Y chains therefore simply could be shorter P polymer chains. Therefore, a differentiation between P and Y chains could no longer be distinguished. However, an argument exists counter to such an assumption. Recently, absorption spectra[8] of oligomers in TS/FBS crystals have been reported. None of the absorption bands belonging to the short chains of stable oligomers do coincide with the Y absorption. Therefore, an assignment of the Y absorption to any short polymer chain is not possible.

Recently, Batchelder and co-workers[39,40] reported that structural phase transitions occurred when oxygen was adsorbed by PDA single crystals. They found differences in Raman spectra between PDA crystals with and without oxygen adsorbed, which are very similar to those which we found for Y and P zones. Three main arguments are against an assumption that oxygen adsorption could be the reason for the Y zones. First, no absorption comparable to the Y absorption could be found for PDA crystals with oxygen adsorbed. Second, there would be no explanation for the sharp separation of the color zones. Adsorption should be more homogeneous. Third, it was found that the structural change was reversible upon removal of the oxygen under vacuum. In all our experiments we placed the freshly cleaved TS/FBS crystals into a cryostat which had been evacuated. These facts support that the Y zones are not caused by any kind of adsorption.

Other observations provide important clues as to an explanation of the nature of the Y zones. Investigations of PDA and DA crystals containing defects showed that luminescence (not as structured but similar to that shown in Fig. 7) occurred upon irradiation by blue light near defects.[8,41] Fluorescence spectroscopy on FBS DA oligomers[42] yielded structured spectra which are comparable to spectra displayed in Fig. 7. On the other hand, defect free PDA crystals, containing long polymer chains, do not show remarkable luminescence. An observation made for DA crystals

containing color zones, in fact, points to defects as the proper cause of chromism in these crystals. The observation of sharp color zones in DA crystals has first been described for TS/FBS crystals.[9] However, TS6 and, very often, FBS DA crystals show color zones.[8] The appearance of color zones seemed always to depend on the growth condition of the crystals. On the {100} surface of the crystals, typical zones of different roughness could be observed. These surface zones corresponded mostly to the *P* and *Y* zones of the crystals. Various investigations (see Ref. 8 and references therein) showed that edge dislocations are preferrably situated in {111} growth sectors. A strain field is forced upon neighboring monomer molecules by small-angle grain boundaries formed by dislocations having a Burgers vector in the *b* direction ([010]). As a consequence, these crystal defects most probably influence the side groups of the polymer chains which results in a change of the conjugation of the π-electron system. This even may lead to interruptions of the conjugation lengths and therefore to higher absorption frequencies. Recently, Eckardt *et al.*[19] used valence effective Hamiltonian (VEH) and modified neglect of diatomic overlap (MNDO) calculations to explain the influence of side-group angle relative to the PDA backbone on optical properties of PDA's. They suggested that the energy shift to higher frequencies of the absorption as well as stretching vibrations in PDA's can be understood in terms of strain unduced by substituents. These authors found that side-group distortions needed to produce shifts, seen for chromatic transitions, require only a subtle rearrangement of backbone geometry. Crystal defects therefore could effect the building of *Y* zones, even when they only represent a slight hindrance for the side groups. There were different frequencies found for color zones of DA's with different substituents.[20] This strongly points to a main role of side-group geometry for chromism in these DA crystals. Tomioka *et al.*[43] investigated the surface-pressure-induced reversible color change of a polydiacetylene monolayer at a gas–water interface. They gave a rather simplified expression for the influence of side-group geometry on the electronic properties of conjugated backbones of polymer chains. This description originates from a one-electron tight-binding approach to the Hückel molecular orbital description on finite carbon chains. The energy of the band gap for a nonplanar polymer backbone (E_{bg}) differs from that of the all-planar case (E^0_{bg}) according to

$$E^0_{bg} - E_{bg} = \Delta_{tors}, \tag{4}$$

where Δ_{tors} is the energy shift caused by a torsion around the C–C single bond in the acetylenic backbone structure. Δ_{tors} is given by

$$\Delta_{tors} = 2t^0_{ij}(\cos\phi \exp\{-\Delta r_{ij}/a\} - 1). \tag{5}$$

t^0_{ij} arises from the hopping integrals between the nearest-neighbor unit cells *i* and *j* and is proportional to the bandwidths of the valence and conduction bands. ϕ corresponds to the dihedral angle around the C–C single bond in the acetylenic backbone structure (see Fig. 1). $\Delta r_{ij}/a$ is the normalized change of the distance between neighbor unit cells *i* and *j* and therefore represents the change in bond lengths in the polymer chains. From our resonance Raman and CARS spectra we know that the C=C and the C≡C stretching vibrations shift to higher frequencies for the *Y* chains. Experiments were performed which investigated the pressure dependence of the electronic and vibrational excitations of a conjugated polymer crystal.[44] They showed that such anti-Stokes shifts of the vibrational frequencies arise from a decrease in chain length. Thus $\exp\{-\Delta r_{ij}/a\}$ increases as a result of the transition from *P* to *Y* chains. A shortening of the chains alone, however, would not explain a shift of the absorption to higher energies. This means that $t^0_{ij}\cos\phi$ must decrease which implies a distortion of planarity in the conjugated backbone structure. Slight rotations around the single bonds of the conjugated backbone lead to a decreasing $\cos\phi$ and at the same time to a weaker conjugation. This results in a decrease of t^0_{ij}, as well. If we suppose that the {111} growth sectors are identical with the observed color zones and take into account the aforementioned discussion we obtain a rather complete explanation for the origin of color zones in DA crystals.

IV. CONCLUSION

Color effects seem to be a general property of DA polymer chains. The simultaneous occurrence of two well separated color forms in TS/FBS, FBS, and TS6 DA crystals motivated us to investigate the origin of these color zones in detail. Simultaneous information from absorption, luminescence, resonance Raman, and CARS spectroscopy were used to interpret the nature of color zones. The absorption spectroscopy gave us the possibility to characterize the color shift. The absorption spectra showed different resolved vibronic structure of the polymer chains in the DA crystals. This effect has been explained by applying a NFEM theoretical model, assuming that different growth conditions result in different chain length distributions. Because of the strong luminescence occuring in the *Y* zones, we could not gain much new information out from resonance Raman spectroscopy. Anti-Stokes Raman spectroscopy was not possible to perform because of the high sensitivity of the DA crystals toward laser intensities. Resonance CARS spectroscopy as an anti-Stokes and, therefore the luminescence free method, has been shown to be an excellent tool to obtain Raman data. In spite of some problems caused by the photosensitivity of the DA crystals, we gained sufficient information by this spectroscopic method concerning the nature of *Y* chains. In combination with observations of defect structures associated with the color zones, we were able to explain the origin of these color zones. {111} growth sectors containing edge dislocations perturb the side-group geometry in the DA crystals. The shift of absorption and Raman lines to higher frequencies could be explained by a simple theoretical model. The torsion of the side groups leads to a disturbance of the planarity of the polymer backbone. This results in an increase of both the absorption and the vibrational energy. This model also explains the strong influence of the DA substituents on the chromisms.

We have shown the advantageous use of CARS spectroscopy for the investigation of DA's. Resonance CARS can be a good tool for examination of electronic as well as structural properties of systems which are not accessible by

linear resonance Raman spectroscopy. Up to now, only very little work in CARS spectroscopy on absorbing solids has been reported. Two main reasons prevented such measurements in the past. First, many materials are destroyed by the heat resulting from absorption of the exciting laser wavelengths. The second problem is that the conventional CARS arrangement is set up for transmission measurements. Very often, strongly absorbing samples cannot be made as thin enough layers to transmit the CARS signal. To overcome this problem, the materials under investigation could be dispersed in a nonabsorbing matrix, or a backscattering CARS arrangement as proposed by Pfeiffer *et al.*[45] could be used. The latter method would allow many new applications of CARS spectroscopy such as investigations on PDA crystals.

ACKNOWLEDGMENTS

We thank Mrs. Irene Müller, University of Bayreuth, for growing excellent samples of TS/FBS DA crystals. One of us (A. M.) thanks the Stiftung Volkswagenwerk and the Fonds der Chemischen Industrie for a postgraduate scholarship. Financial support by the Fonds der Chemischen Industrie e.V. and the German Science Foundation (SFB 347, project C-2) is highly acknowledged.

[1] *Conjugated Polymeric Materials: Opportunities in Electronics, Optoelectronics, and Molecular Electronics,* Vol. 182 of NATO *Advanced Study Institute Series E,* edited by J. L. Brédas and R. R. Chance (Kluwer, Dordrecht, 1990).
[2] C. Sauteret, J.-P. Hermann, R. Frey, F. Pradére, J. Ducuing, R. H. Baughman, and R. R. Chance, Phys. Rev. Lett. **36**, 956 (1976).
[3] G. Wegner, Z. Naturforsch. B **24**, 824 (1969).
[4] P. Strohriegl, Makromol. Chem., Rapid Commun. **8**, 437 (1987).
[5] M. Bertault, L. Toupet, J. Canceill, and A. Collet, Makromol. Chem. **8**, 443 (1987).
[6] G. Wegner, in *Molecular Metals*, edited by W. E. Hatfield (Plenum, New York, 1979).
[7] V. Enkelmann, Makromol. Chem. **184**, 1945 (1983).
[8] H.-D. Bauer, A. Materny, I. Müller, and M. Schwoerer, Mol. Cryst. Liq. Cryst. **200**, 205 (1991).
[9] A. Materny, H.-D. Bauer, P. Strohriegl, and M. Schwoerer, Verhandl. DPG (VI) **23**, M-7.2 (1988).
[10] R. H. Austin, G. L. Baker, S. Etemad, and R. Thompson, J. Chem. Phys. **90**, 6642 (1989).
[11] M. A. Taylor, J. A. Odell, D. N. Batchelder, and A. J. Campbell, Polymer **31**, 1116 (1990).
[12] G. J. Exarhos, W. M. Risen, Jr., and R. H. Baughman, J. Am. Chem. Soc. **98**, 481 (1976).
[13] H. Tanaka, M. A. Gomez, A. E. Tonelli, A. J. Lovinger, D. D. Davis, and M. Thakur, Macromolecules **22**, 2427 (1989).
[14] G. Lieser, B. Tieke, and G. Wegner, Thin Solid Films **68**, 77 (1980).
[15] M. Wenzel and G. H. Atkinson, J. Am. Chem. Soc. **111**, 6123 (1989).
[16] T. Hasegawa, K. Ichikawa, T. Kanetake, T. Koda, K. Takeda, H. Kobayashi, and K. Kubodera, Chem. Phys. Lett. **171**, 239 (1990).
[17] D. J. Sandman, Mol. Cryst. Liq. Cryst. **189**, 273 (1990).
[18] R. R. Chance, R. H. Baughman, H. Müller, and C. J. Eckardt, J. Chem. Phys. **67**, 3616 (1977).
[19] H. Eckhardt, D. S. Boudreaux, and R. R. Chance, J. Chem. Phys. **85**, 4116 (1986).
[20] A. Materny and W. Kiefer, Macromolecules (to be published).
[21] A. Materny and W. Kiefer, Verhandl. DPG (VI) **26**, 764 (1991).
[22] M. Ganz, W. Kiefer, A. Materny, and P. Vogt, J. Mol. Struct. **266**, 115 (1992).
[23] A. Materny, M. Schwoerer, and W. Kiefer, in *Proceedings of the XIIth International Conference on Raman Spectroscopy*, edited by J. R. Durig and J. F. Sullivan (Wiley, Chichester, 1990), p. 742.
[24] A. Materny, M. Leuchs, T. Michelis, K. Schaschek, and W. Kiefer, J. Raman Spectrosc. **23**, 99 (1992).
[25] D. Bloor, F. H. Preston, and D. J. Ando, Chem. Phys. Lett. **38**, 33 (1976).
[26] H. Sixl, in *Polydiacetylenes*, Vol. 63 of Advances of Polymer Science, edited by H. J. Cantow (Springer, Berlin, 1984), p. 49.
[27] R. Warta, Ph.D. thesis, University of Stuttgart, 1989.
[28] *Polydiacetylenes, Vol. 102 of NATO Advanced Study Institute Series E,* edited by D. Bloor and R. R. Chance (Nijhoff, Dordrecht, 1985).
[29] D. Bloor, F. H. Preston, D. J. Ando, and D. N. Batchelder, in *Structural Studies of Macromolecules by Spectroscopic Methods*, edited by K. J. Ivin (Wiley, Chichester, 1976), p. 91.
[30] D. N. Batchelder and D. Bloor, J. Phys. C **15**, 3005 (1982).
[31] D. N. Batchelder and D. J. Bloor, J. Polym. Sci. Polym. Phys. Ed. **17**, 569 (1979).
[32] L. X. Zheng, R. E. Benner, and Z. V. Vardeny, Synth. Met. **41-43**, 235 (1991).
[33] S. A. J. Druet and J.-P. E. Taran, Progr. Quant. Electr. **7**, 1 (1981).
[34] *Non-Linear Raman Spectroscopy and Its Chemical Applications*, edited by W. Kiefer and D. A. Long (Reidel, Dordrecht, 1982).
[35] L. A. Carreira and M. L. Horovitz, *Non-Linear Raman Spectroscopy and Its Chemical Applications*, Ref. 34, p. 367.
[36] L. A. Carreira, L. P. Goss, and T. B. Malloy, Jr., in *Chemical Applications of Nonlinear Raman Spectroscopy*, edited by H. B. Harvey (Academic, London, 1981), Chap. 8, p. 321.
[37] K. C. Lim, M. Sinclair, S. A. Casalnuovo, C. R. Fincher, F. Wudl, and A. J. Heeger, Mol. Cryst. Liq. Cryst. **105**, 329 (1984).
[38] M. A. Müller, M. Schmidt, and G. Wegner, Makromol. Chem. **5**, 83 (1984).
[39] D. N. Batchelder, N. J. Poole, and D. Bloor, Chem. Phys. Lett. **81**, 560 (1981).
[40] B. E. J. Smith and D. N. Batchelder, Polymer **32**, 1761 (1991).
[41] H. Eichele and M. Schwoerer, Phys. Status Solidi A **43**, 465 (1977).
[42] R. Warta and H. Sixl, J. Chem. Phys. **88**, 95 (1988).
[43] Y. Tomioka, N. Tanaka, and S. Imazeki, J. Chem. Phys. **91**, 5694 (1989).
[44] A. C. Cottle, W. F. Lewis, and D. N. Batchelder, J. Phys. C **11**, 605 (1978).
[45] M. Pfeiffer, A. Lau, and W. Werncke, J. Raman Spectrosc. **21**, 835 (1990).